Science of the Total Environment 825 (2022) 153823

Contents lists available at ScienceDirect

Science of the Total Environment

journal homepage: www.elsevier.com/locate/scitotenv

Influences of impervious surfaces on ecological risks and controlling strategies in rapidly urbanizing regions

Ying Hou [a,b], Wenhao Ding [a,b], Changfeng Liu [c], Kai Li [d], Haotian Cui [a,b], Baoyin Liu [e], Weiping Chen [a,b,*]

[a] State Key Laboratory of Urban and Regional Ecology, Research Center for Eco-Environmental Sciences, Chinese Academy of Sciences, Beijing 100085, China
[b] University of Chinese Academy of Sciences, Beijing 101408, China
[c] Beijing Qingyuan Eco-environmental Co., LTD, Beijing 102200, China
[d] Department of Geosciences and Natural Resources Management, University of Copenhagen, Copenhagen DK 1165, Denmark
[e] Institutes of Science and Development, Chinese Academy of Sciences, Beijing 100190, China

HIGHLIGHTS

- We analyzed the spatial-temporal dynamics of the ecological risks in Beijing.
- We proposed the risk control strategies based on impervious surface influences.
- Ecological risks were low in the mountainous areas and high on the plain areas.
- The impervious surface sprawl mainly caused the large ecological risk increases.
- Differentiated risk control strategies are needed for distinct strategy categories.

GRAPHICAL ABSTRACT

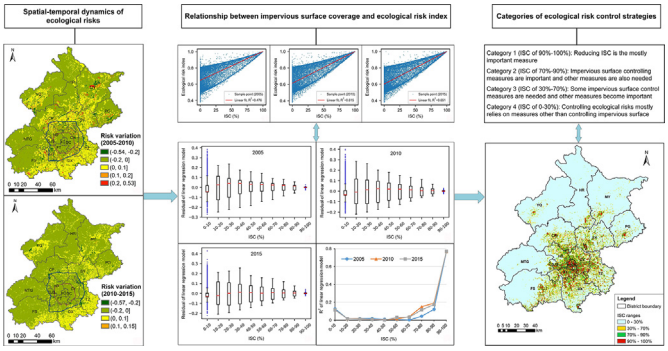

ARTICLE INFO

Article history:
Received 28 November 2021
Received in revised form 8 February 2022
Accepted 8 February 2022
Available online 11 February 2022

Editor: Fernando A.L. Pacheco

Keywords:
Ecosystem services
Equivalent factor
Spatial-temporal dynamics
ISC: impervious surface coverage
Thresholds
Categorization

ABSTRACT

Reducing ecological risks is important for promoting regional sustainable development. However, studies on the influence of impervious surfaces on ecological risks and risk control strategies in regions undergoing rapid urbanization are limited. Therefore, this study aimed to demonstrate the spatial-temporal dynamics of regional ecological risks using Beijing as a case study to reveal the influence of impervious surfaces and explore the controlling strategies of risks. We first characterized the ecological risks in Beijing based on the ecosystem service values and mapped the risk levels and temporal variations in risks. We then identified the ecological risk increases caused by impervious surface expansion and built linear regression models for impervious surface coverage (ISC) and risk index. Finally, we formulated ecological risk control strategies for the strategy categories identified based on the ISC thresholds. The results show that the mountainous areas mainly exhibited low ecological risk levels, and the plain areas mainly showed high levels. The expansion of impervious surface was the main cause of the relatively large temporal increase in ecological risks from 2005 to 2015. Moreover, the strategies for ecological risk control can be divided into four categories based on the division of ISC, with 30%, 70%, and 90% as the thresholds. For risk control strategies, reducing ISC is the most important measure to reduce ecological risks for the category with an ISC range of 90%–100%, and increasing the area proportions of forests and water bodies is the most effective measure for the category with an ISC range of 0%–30%. For the other two categories, controlling the ISC and other strategies are required. Our study can increase the understanding of the influences of impervious surfaces on ecological risks in rapidly urbanizing regions and help inform the formulation of strategies for controlling the ecological risks in Beijing.

* Corresponding author at: State Key Laboratory of Urban and Regional Ecology, Research Center for Eco-Environmental Sciences, Chinese Academy of Sciences, Beijing 100085, China.
E-mail address: wpchen@rcees.ac.cn (W. Chen).

http://dx.doi.org/10.1016/j.scitotenv.2022.153823

1. Introduction

Rapid urbanization has caused significant ecosystem service losses and, consequently, a large increase in ecological risk in many regions (Kang et al., 2019). The ecological effects and regional ecological risks have become hot research topics for regional sustainable development, and the control of ecological risks has become an important concern for managers in many regions (Bai et al., 2014; Kang et al., 2018; Lü et al., 2018). The rapidly urbanizing regions are complex socioecological systems with high spatial-temporal heterogeneity in the patterns, processes, and functions of ecosystems and socioeconomic activities. There are multiple influences on the development of such complex systems, from natural processes and human activities (Young et al., 2006; Collins et al., 2011; Wang and Ouyang, 2012). Therefore, to achieve the sustainable development of rapidly urbanizing regions, revealing the spatial-temporal dynamics of ecological risks, demonstrating the influential factors, and developing rational risk control strategies in these regions are important.

Methods for evaluating regional ecological risks based on ecosystem services have been developed. For example, Kang et al. (2019) developed a method to characterize regional ecological risks based on ecosystem services values (ESVs), and Wang et al. (2021) evaluated ecological risks from the perspective of the relationship between ecosystem service supply and demand. Studies have shown large spatial-temporal dynamics of ecological risks in some regions. Considerable spatial variations in ecological risks have been found in different types of regions, such as mountainous areas (Qi et al., 2020; Wang et al., 2021) and river basins (Bartolo et al., 2012; Heenkenda and Bartolo, 2016). High ecological risks often occur in areas with high-intensity human activities (Qi et al., 2020; Yang et al., 2020; Wang et al., 2021). For example, the comprehensive ecological risk index values were high in areas with many instances of agricultural and industrial production and urban land use in Wei River Basin, China (Yang et al., 2020). Large temporal dynamics of ecological risks have also been reported, showing that the risk level increased mainly in areas under rapid urbanization (Kang et al., 2018; Yang et al., 2018; Wang et al., 2021). Moreover, some studies have demonstrated that ecological risks can be reduced in future scenarios in which optimal regional plans are implemented (Luo et al., 2021).

As a widely used proxy of the urbanization level, impervious surface coverage (ISC) is often used to analyze the influence of urbanization on ecological processes and functions associated with ecological risks. Studies have found that an increase in ISC increases the land surface temperature in urban areas (Xu et al., 2013; Zhang et al., 2015; Kuang et al., 2018), runoff in urban areas and watersheds (Schuele, 1994; Bian et al., 2017; Bell et al., 2019; Liu et al., 2020), and water environmental degradation in watersheds (Dietz and Clausen, 2008; Meierdiercks et al., 2017). Habitat quality and biodiversity are also negatively correlated with ISC (Schuele, 1994; Walsh and Webb, 2016; Xie et al., 2018a). Moreover, some studies, such as those by Liao et al. (2017) in Xiamen City and Kang et al. (2019) in the Beijing–Tianjin–Hebei urban agglomeration, have reported that the expansion of impervious surfaces causes losses of ecosystem services, increasing ecological risk.

ISC thresholds exist widely in terms of the influence of impervious surfaces on ecological risks. For example, there are thresholds of 40%–60% for the positive impact of ISC on the urban heat island effect in Tampa Bay, United States (Xian and Crane, 2006). Another example is that the ISC threshold for stream ecosystem degradation is approximately 10% in southeastern Wisconsin, United States (Wang, 2007). In addition to ISC, the spatial pattern of impervious surfaces has been found to affect land surface temperature, runoff, and ecosystem quality (Alberti et al., 2007; Estoque et al., 2017; Su and Duan, 2017). For example, the mean patch size and aggregation index of impervious surfaces are highly positively correlated with land surface temperature and highly negatively correlated with in-stream biotic integrity in highly urbanized areas (Alberti et al., 2007; Estoque et al., 2017). Despite findings on the influence of impervious surfaces on ecosystems, there is limited research on the impact of impervious surfaces on the comprehensive ecological risks in rapidly urbanizing regions.

Some studies have proposed strategies to control the adverse environmental and ecological effects associated with ecological risks. Differentiating the ecological risk control strategies for different management categories is an essential step for regions with large risk changes (Schuele, 1994; Meng et al., 2015; Yang et al., 2016). For example, distinguished countermeasures of ecological risk management have been proposed for varying degrees of risk in Ordos, China (Meng et al., 2015), and for different function zones in Sheyang, China (Yu et al., 2016b). Controlling ISC is an important strategy for areas exhibiting apparent adverse effects of impervious surfaces, such as surface runoff (Yu et al., 2019) and water environments (Yang et al., 2016). Moreover, studies have proposed landscape configuration strategies, such as fitting streetscapes with tree-based stormwater control measures to reduce stormwater runoff (Thom et al., 2020) and evenly distributing land use types to decrease urban flood risks (Wu and Zhang, 2017). Despite the countermeasures provided in the literature to reduce adverse environmental or ecological effects, studies proposing strategies for ecological risk control in rapidly urbanizing regions are limited.

Based on the aforementioned identified knowledge gaps, our study aimed to 1) demonstrate the spatial-temporal dynamics of ecological risks and the influences of impervious surfaces in rapidly urbanizing regions and 2) explore the strategies for controlling regional ecological risk. To achieve these objectives, we implemented a case study of Beijing, a typical region that has experienced rapid urbanization in the past decades. Our work can increase the understanding of the influences of impervious surfaces on regional ecological risks and provide insights into ecological risk control in rapidly urbanizing regions.

2. Study area and methods

2.1. Study area

Beijing is the capital and municipality under the direct administration of the central government of China. In its northern part is the Yan Mountains, in its western part is the Taihang Mountains, and the remainder is in the North China Plain (within 115.7° E–117.4° E, 39.4° N–41.6° N). Beijing has an area of 16,410.5 km^2, with the mountainous areas accounting for approximately 62% and the plain areas accounting for approximately 38%. Beijing has a typical temperate semi-humid continental monsoon climate with hot weather and high precipitation in summer and cold, dry weather in winter. This region has an annual average precipitation of 483.9 mm and an annual average temperature of 11 °C–13 °C.

Beijing has experienced rapid urbanization, for example, the urban population increased from 12.86 million in 2005 to 18.77 million in 2015 (increased by 46%, Chen et al., 2018). The rapid urbanization during this period increased the impervious surface area by 16.08%, mainly in the form of urban expansion (Fig. 1). Urban expansion has exacerbated environmental and ecological problems, such as urban floods, urban heat island effects, air pollution, aquatic ecosystem degradation, and biodiversity loss (Lü et al., 2018). Therefore, Beijing represents a typical case area for studying ecological risks in regions undergoing rapid urbanization.

2.2. Methods

2.2.1. Analysis of ecological risks

2.2.1.1. Ecological risk characterization

2.2.1.1.1. Ecological risk index calculation. Ecosystem services reflect ecosystem conditions and health and are crucial for human well-being. Regional ecological risk assessments are important for policymakers aiming to develop policies that protect regional ecological features and social values (Graham et al., 1991). Therefore, regional ecological risk assessment based on the ecosystem service approach has clear management implications for sustainable regional development in social-ecological systems (Wang et al., 2021). Considering the linkage between ecosystem services and regional ecological risks, we developed a comprehensive index that

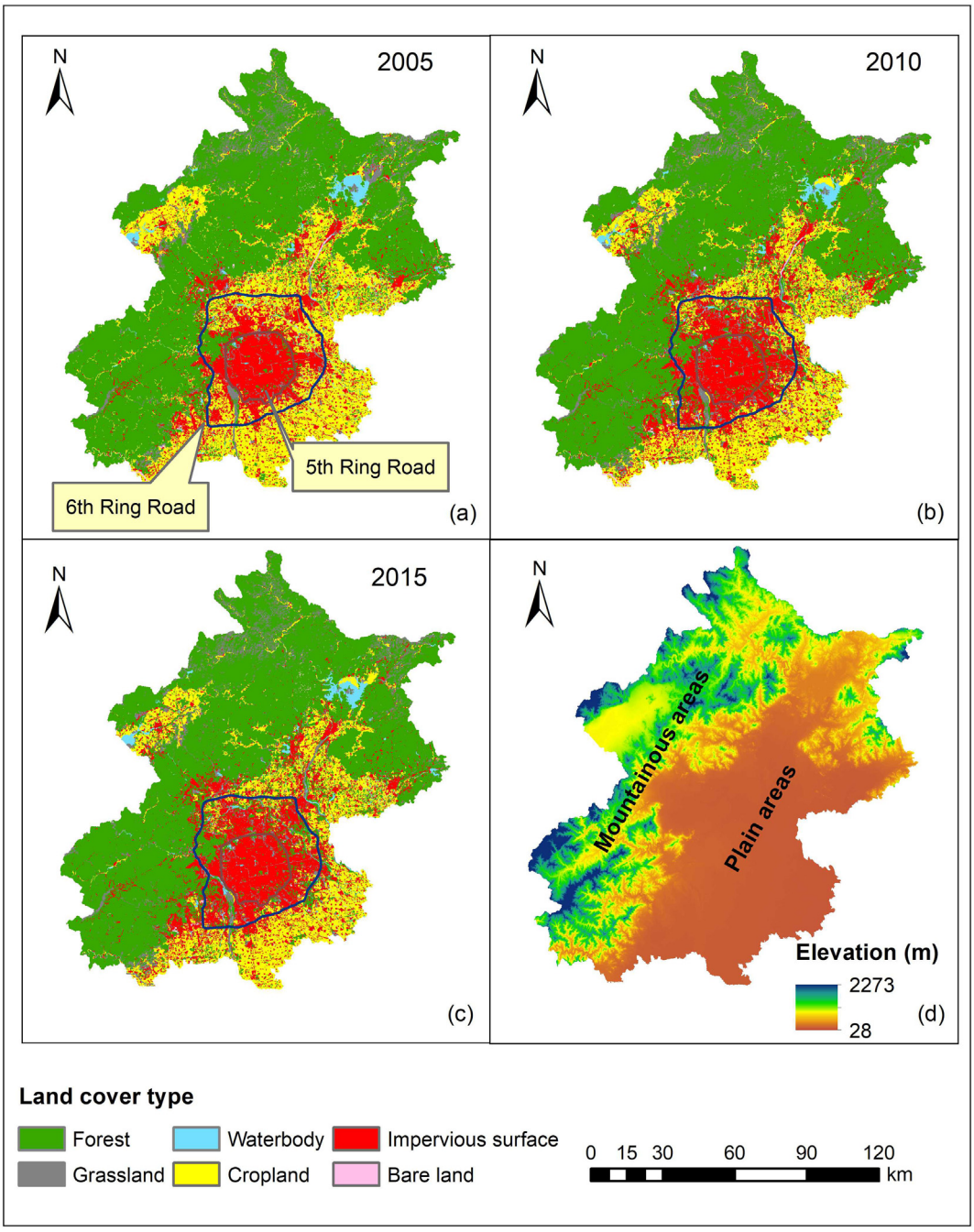

Fig. 1. Spatial patterns of land covers and elevation in Beijing. Landsat TM remote sensing data were used for land cover classification (See Yu et al., 2016a).

reflects the relative loss of ecosystem services to characterize ecological risks in rapidly urbanizing regions by using the Technique for Order Preference by Similarity to Ideal Situation method (Izadikhah et al., 2014; Yang et al., 2020) in this study. First, we used all the spatial units (e.g., pixels of raster data) in the study area in 2005, 2010, and 2015 as the sample. Using the sample, we created a hypothesized "positive ideal sample point" and a hypothesized "negative ideal sample point" in which all ecosystem service types exhibit the highest and lowest values, respectively, in the entire study area in the three years. Second, we used the ESV of the "positive ideal sample point" as the threshold of ecological risk and calculated the largest ecosystem service loss as the Euclidean distance of the ESV from the "positive ideal sample point" to the "negative ideal sample point." Third, we calculated the Euclidean distance of the ESV from the real sample point to the "positive ideal sample point." Finally, we calculated the ecological risk index as the ratio of these two Euclidean distances.

The specific calculation method for the ecological risk index is as follows:

First, we calculated the values of n ecosystem service types of m spatial sample points (m pixels in this case study) by using an evaluation method (the method is explained in the next subsection) and created a matrix of ESV using all the spatial sample points (Eq. (1)):

$$ESV = \begin{bmatrix} esv_{11} & esv_{12} & \cdots & esv_{1n} \\ esv_{21} & esv_{22} & \cdots & esv_{2n} \\ \cdots & \cdots & \vdots & \cdots \\ esv_{m1} & esv_{m2} & \cdots & esv_{mn} \end{bmatrix} \quad (1)$$

where ESV is the matrix of ESV, and esv_{mn} is the value of ecosystem service type n of spatial sample point m.

To eliminate the influences of dimension and order of magnitude, we normalized the matrix of the ESV by using Eq. (2):

$$r_{ij} = \frac{esv_{ij} - min\left(esv_{\bullet j}\right)}{max\left(esv_{\bullet j}\right) - min\left(esv_{\bullet j}\right)} \tag{2}$$

where r_{ij} is the normalized value of ecosystem service type j of sample point i, $max(esv_{\bullet j})$ is the maximum value of ecosystem service type j in the entire sample, $min(esv_{\bullet j})$ is the minimum value of ecosystem service type j in the entire sample, and esv_{ij} is the value of ecosystem service type j of sample point i.

Second, we created a weighted matrix of ecosystem services for the entire sample by using Eq. (3):

$$Y = \begin{bmatrix} y_{11} & y_{12} & \cdots & y_{1n} \\ y_{21} & y_{22} & \cdots & y_{2n} \\ \cdots & \cdots & \vdots & \cdots \\ y_{m1} & y_{m2} & \cdots & y_{mn} \end{bmatrix} = \begin{bmatrix} \omega_1 r_{11} & \omega_2 r_{12} & \cdots & \omega_n r_{1n} \\ \omega_1 r_{21} & \omega_2 r_{22} & \cdots & \omega_n r_{2n} \\ \cdots & \cdots & \vdots & \cdots \\ \omega_1 r_{m1} & \omega_2 r_{m2} & \cdots & \omega_n r_{mn} \end{bmatrix} \tag{3}$$

where Y is the weighted matrix, y_{mn} is the weighted normalized value of ecosystem service type n of sample point m, ω_n is the weight of ecosystem service type n, and r_{mn} is the normalized value of ecosystem service type n of sample point m.

Third, the positive and negative ideal sample points were created as

$$y^+ = [\,max\,(y_{\bullet 1}) \;\; max\,(y_{\bullet 2}) \;\; \cdots \;\; max\,(y_{\bullet n})] \tag{4}$$

$$y^- = [\,min\,(y_{\bullet 1}) \;\; min\,(y_{\bullet 2}) \;\; \cdots \;\; min\,(y_{\bullet n})\,] \tag{5}$$

in which y^+ means the "positive ideal sample point," y^- means the "negative ideal sample point", $max(y_{\bullet n})$ means the maximum weighted normalized value of ecosystem service type n in the entire sample, and $min(y_{\bullet n})$ means the minimum weighted normalized value of ecosystem service type n in the entire sample.

Fourth, we calculated the relative loss of ecosystem services as

$$D_i^+ = \sqrt{\sum_{j=1}^{n}\left(max\left(y_{\bullet j}\right) - y_{ij}\right)^2} \tag{6}$$

$$D_{max}^+ = \sqrt{\sum_{j=1}^{n}\left(max\left(y_{\bullet j}\right) - min\left(y_{\bullet j}\right)\right)^2} \tag{7}$$

where D_i^+ means the Euclidean distance of the ESV between sample point i and the "positive ideal sample point," D_{max}^+ means the Euclidean distance of ESV between the positive and the negative ideal sample points, indicating the distance at which the relative loss of ESV reaches the highest; $max(y_{\bullet j})$ means the maximum weighted normalized value of ecosystem service type j in all the sample points; $min(y_{\bullet j})$ means the minimum weighted normalized value of ecosystem service type j in all the sample points; and y_{ij} means the weighted normalized value of ecosystem service type j of sample point i.

Fifth, we calculated the ecological risk index as

$$R_i = \frac{D_i^+}{D_{max}^+} \tag{8}$$

where R_i is the ecological risk index of sample point i, whose value range is 0–1. The closer the index value is to zero, the smaller the relative ESV loss and the lower the ecological risk. By contrast, the closer the index value is to one, the larger the relative ESV loss and the higher the ecological risk.

2.2.1.1.2. Ecosystem services evaluation and determination of weights. This study used the equivalent factor method, which belongs to the unit value-based approach (Costanza et al., 1997), to calculate the value of ecosystem services (Xie et al., 2017). Using this method, the ESV was calculated as follows:

$$esv_{ij} = E \times \sum_{k=1}^{6}\left(D_{jk} \times A_{ik}\right) \tag{9}$$

where esv_{ij} is the value of ecosystem service type j of spatial sample point i, and E is the monetary value of an equivalent factor (RMB Yuan/hm^2), which is the economic value of annual natural food production provided by 1 hm^2 cropland with national average productivity. For the value of this variable, we referred to Xing et al. (2020) and used the annual average value of the net profit of crops in China from 2005 to 2015 published in the Compilation of National Agricultural Product Cost and Benefit Data of China (2005–2015), where A_{ik} denotes the area of land cover type k (hm^2) in region i (pixel i in this case study), and D_{jk} denotes the equivalent factor of ecosystem service type j provided by land cover type k.

We used the equivalent factors of nine ecosystem service types provided by different land cover types in Xie et al. (2008) (Table 1). To obtain equivalent factors suitable for Beijing, we modified the factors based on precipitation and the Normalized Difference Vegetation Index (NDVI) by referring to Xie et al. (2017) and Shi et al. (2012). The NDVI is an indicator of vegetation greenness, which is interpreted from remote sensing images and calculated from the visible and near-infrared light reflected by vegetation. The method used to modify the equivalent factors is described in the Supplementary Material. Moreover, to differentiate the importance of the ecosystem service types, we calculated the weight of the nine ecosystem service types using the entropy weight method (Xie et al., 2018b) described in the Supplementary Material. The ESV and ecological risk index values were calculated using ArcGIS 10.5.

Data used to calculate ecosystem service values and ecological risks are listed in Table S1 in the Supplementary Material.

2.2.1.2. Analysis of spatial-temporal changes in ESV and ecological risks. Based on the ESV evaluations described in the prior subsection, we calculated the differences in ESV between 2005 and 2010 and between 2010 and 2015 in Beijing. Moreover, based on the ecological risk index calculated, we categorized the risk in 2005, 2010, and 2015 in Beijing into five levels by using the Jenks Natural Breaks method and then created the maps of risk levels for the three years to show the spatial variations in ecological risks. Furthermore, we mapped the temporal variation in ESV and risks for two periods (2005–2010 and 2010–2015). The risk variations were calculated as the differences in the ecological risk index values between 2005 and 2010

Table 1
Equivalent factors of ecosystem service types (referring to Xie et al., 2008) and the weights.

ES classification	ES types	Forest	Grassland	Cropland	Waterbody	Impervious surface	Barren land	Weight
Provisioning services	Food supply	0.33	0.43	1.0	0.36	0	0.02	0.1107
	Raw material supply	2.98	0.36	0.39	0.24	0	0.04	0.1104
Regulating services	Air quality regulation	4.32	1.50	0.72	2.41	0	0.06	0.1140
	Climate regulation	4.07	1.56	0.97	13.55	0	0.13	0.1144
	Water flow regulation	4.09	1.52	0.77	13.44	0	0.07	0.1119
	Waste treatment	1.72	1.32	1.39	14.40	0	0.26	0.1119
	Soil retention	4.02	2.24	1.47	1.99	0	0.17	0.1107
Supporting services	Biodiversity maintenance	4.51	1.87	1.02	3.69	0	0.40	0.1103
Cultural services	Recreation	2.08	0.87	0.17	4.69	0	0.24	0.1107

and between 2010 and 2015. To show the temporal changes in the ecological risks in each district and then compare the districts, we calculated the mean values of the ecological risk index for each district for the three years and created bar charts of the risk index values. The calculations and mappings were performed using ArcGIS 10.5, and bar charts were created using Excel.

2.2.2. Analysis of the influences of impervious surfaces

2.2.2.1. Identifying ecological risk increases caused by impervious surface expansion. First, we categorized the increases in ecological risks into two levels (0–0.1 and over 0.1) for 2005–2010 and 2010–2015. Second, we calculated the area of the pixels where ecological risks increased by two levels in the two periods. Among the pixels where ecological risk increased, we further calculated the area proportions of the land cover types converted to impervious surface. These area proportions reflect the degree to which the ecological risk increases were caused by impervious surface expansion. Calculations were performed using ArcGIS 10.5.

2.2.2.2. Analysis of the relationship between ISC and the ecological risk index. We created scattered graphs and built weighted linear regression models to explore the relationship between ISC and the ecological risk index in 2005, 2010, and 2015. For each year, to reduce the sample size, we used a sample of 1 km × 1 km pixels of Beijing instead of the 30 m × 30 m pixels. The 1 km resolution ISC data were calculated based on the spatial data on land cover with a 30 m resolution by using ArcGIS 10.5. To be specific, the ISC was calculated as the proportion of the number of 30 m × 30 m pixels of impervious surface in a 1 km × 1 km cell to the total number of pixels in the cell. The 30 m resolution impervious surface spatial data were derived based on land cover classification using the Landsat TM remote sensing data. The 1 km resolution risk index data were generated by resampling the 30 m resolution data. Weighted linear regression models were built by fitting the scatter plots of ISC versus the ecological risk index, using SPSS Statistics 17.0.

2.2.3. Exploration of controlling strategies

2.2.3.1. Categorization of strategies for ecological risk control. On the one hand, the influence of ISC on the environment and ecosystem usually exhibits tipping points (Walsh et al., 2005; Guo et al., 2019); one the other hand, ISC is often the controlling target in the regional environment or ecosystem management, especially in regions undergoing rapid urbanization (Yu et al., 2019). Therefore, we categorized ISC for risk control on the basis of the changes in the accuracy of the linear regression models for the relationship between ISC and the ecological risk index. For the categorization of ISC, we first divided ISC into 10 equal ranges (0–10% to 90%–100%) for 2005, 2010, and 2015. Next, we built linear regression models for each ISC range, constructed box plots of the residuals, and calculated the R^2 of the models for the three years. Finally, we categorized ISC based on the changes in the distributions of the model residuals and the changes in R^2 with the increase in ISC. Different ISC categories exhibit apparent distinct variation trends of residual distributions or R^2 and thus require distinct strategies for ecological risk control. The creation of the box plots of the model residentials and the calculation of the model R^2 were performed using Python 3.7.

2.2.3.2. Proposal of ecological risk control strategies. We proposed categories of strategies for controlling the ecological risk in Beijing on the basis of the division of the ISC ranges: (1) for categories in which the linear correlation between ISC and the ecological risk index is strong, we proposed risk control strategies that mainly target reducing ISC, because reducing ISC is highly likely reduce ecological risk in this situation; (2) for categories in which the linear correlation between ISC and the ecological risk index is moderate, we suggest using both ISC control measures and other measures to reduce ecological risks; and (3) for categories in which the linear correlation between ISC and the ecological risk index is weak, we propose strategies mainly based on measures other than controlling ISC, because reducing ISC is unlikely to reduce ecological risk in this situation.

3. Results

3.1. Spatial-temporal dynamics of ESV and ecological risks in Beijing

3.1.1. Spatial-temporal variations in ESV

The increase in ESV from 2005 to 2010 mainly occurred in the mountainous areas of Beijing, and the value increase was mostly less than or equal to 9.0 × 10^4 Yuan RMB/ha (Fig. 2-a). The plan areas mainly exhibited ESV decreases of less than 3.0 × 10^4 Yuan RMB/ha or no ESV

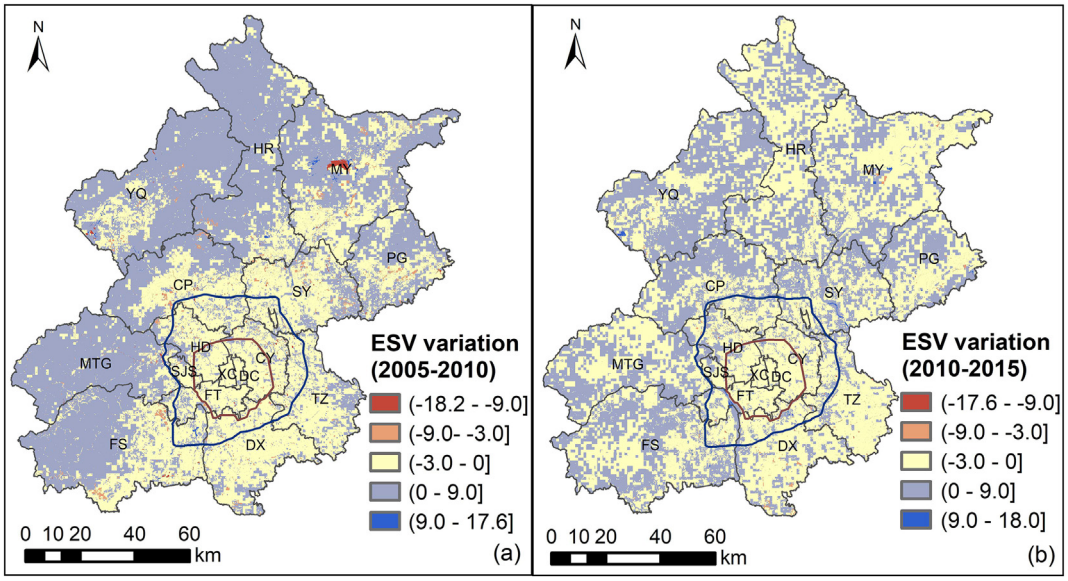

Fig. 2. Variation in ESV (10^4 Yuan RMB/ha) in Beijing for two periods in 2005–2015. The full names of the districts are CP-Changping District, CY-Chaoyang District, DC-Dongcheng District, DX-Daxing District, FS-Fangshan District, FT-Fengtai District, HD-Haidian District, HR-Huairou District, MTG-Mentougou District, MY-Miyun District, PG-Pinggu District, SJS-Shijingshan District, SY-Shunyi District, TZ-Tongzhou District, XC-Xicheng District, and YQ-Yanqing District.

Table 2
Value ranges of ecological risk index for different risk levels and the area proportions of each level in the entire study area.

Ecological risk levels	Risk index value ranges	Area proportions (2005)	Area proportions (2010)	Area proportions (2015)
I (very low)	0.35–0.46	11.24%	24.40%	49.64%
II (low)	0.46–0.59	44.07%	32.43%	8.60%
III (medium)	0.59–0.76	5.11%	6.32%	6.61%
IV (high)	0.76–0.90	23.31%	18.38%	17.00%
V (very high)	0.90–1.0	16.27%	18.46%	18.15%

Note: Risk was categorized using the Jenks Natural Breaks method, in which the samples are all the pixels in 2005, 2010, and 2015. The lowest value of the ecological risk index is not zero, because there is no "positive ideal sample point," which can provide the highest ESV for all service types, in the real world.

variations in this period. Most areas in Beijing also exhibited ESV variation of -3.0×10^4 to 9.0×10^4 Yuan RMB/ha in 2010–2015. However, areas showing an ESV increase or decrease were much more evenly distributed in different districts during this period than in 2005–2010 (Fig. 2-b).

3.1.2. Spatial variations in ecological risks

The ecological risk was categorized into five levels, from very low (level I) to very high (level V), with the risk index value increasing from 0.35 to 1.0 in 2005, 2010, and 2015 in Beijing (Table 2). The high (level IV) and very high (level V) ecological risks were mainly distributed on the plain, on which the areas within the 6th Ring Road exhibited a large area of very high risk. Additionally, the low (level II) and very low (level I) ecological risks were mainly distributed in the mountainous areas in the northern and western parts of Beijing (Fig. 3). Moreover, the area proportion of the very high ecological risk level increased from 16.27% to 18.46% from 2005 to 2010, which mainly occurred between the 5th and 6th Ring Road, and the area proportion of the very low ecological risk level increased from 11.24% to 49.64% from 2005 to 2015, which mainly occurred in the mountainous region.

3.1.3. Temporal variations in ecological risks

Most of the plain areas, except the region within the 6th Ring Road, exhibited ecological risk increases ≤ 0.1 in Beijing from 2005 to 2010 (Fig. 4). In this period, large areas between the 5th and 6th Ring Roads exhibited ecological risk increases of 0.1–0.2. Moreover, most of the mountainous areas and the region within the 5th Ring Road showed ecological risk decreases of -0.2 to 0 in this period. Areas with ecological risk increases were much fewer in 2010–2015 than in 2005–2010. These areas exhibited risk increases of 0–0.1 and were mainly distributed on the cropland in the Yanqing, Miyun, Shunyi, Pinggu, Tongzhou, Daxing, and Fangshan Districts. The remaining areas of Beijing mostly exhibited a risk decrease of -0.2 to 0 in this period.

Regarding temporal variations in the overall ecological risks, the Xicheng, Daxing, Shijingshan, Haidian, and Shunyi Districts showed very small risk increases from 2005 to 2010. However, all districts except the Daxing District showed different degrees of risk decrease from 2010 to 2015 (Fig. 5). The ecological risk in the Daxing District increased by 1.2% from 2005 to 2010 and by 0.1% from 2010 to 2015. Among all districts, seven districts—the Fangshan, Changping, Pinggu, Yanqing, Miyun, Huairou, and Mentougou Districts—exhibited an apparent ecological risk decrease (by over 5%) from 2005 to 2015.

3.2. Influences of impervious surface

The area of pixels where the increase in ecological risk from 2005 to 2010 was ≤ 0.1 was 3898.17 km^2. In this area, only 7.97 km^2 (0.20%) changed from other land cover types to the type of impervious surface in this period (Table 3). However, among the pixels where the increase in ecological risk was over 0.1, 472.55 km^2 (65.29%) were converted from other land cover types to the type of impervious surface. From 2010 to 2015, the proportion of the pixel amount converted from other land cover types to impervious surfaces in the number of pixels with a risk increase over 0.1 was even higher (70.99%). These high proportions indicate that impervious surface expiation was the major cause of the relatively large ecological risk increase (over 0.1) in Beijing from 2005 to 2015.

The weighted linear regression models showed that the ecological risk index exhibited a highly linear relationship with ISC in Beijing, with R^2 values of 0.476, 0.615, and 0.651 for 2005, 2010, and 2015, respectively (Fig. 6). The strength of the positive correlation between the ecological risk index and ISC generally increased as ISC increased.

3.3. Ecological risk control strategies based on ISC

3.3.1. ISC thresholds for categories of ecological risk control strategies

First, residuals of the linear models between ISC and the ecological risk index for each ISC range showed very large variations when ISC was less than 30% in 2005, 2010, and 2015 (Fig. 7-a, −b, −c). This phenomenon means that the linear relationship between ecological risk and ISC is very

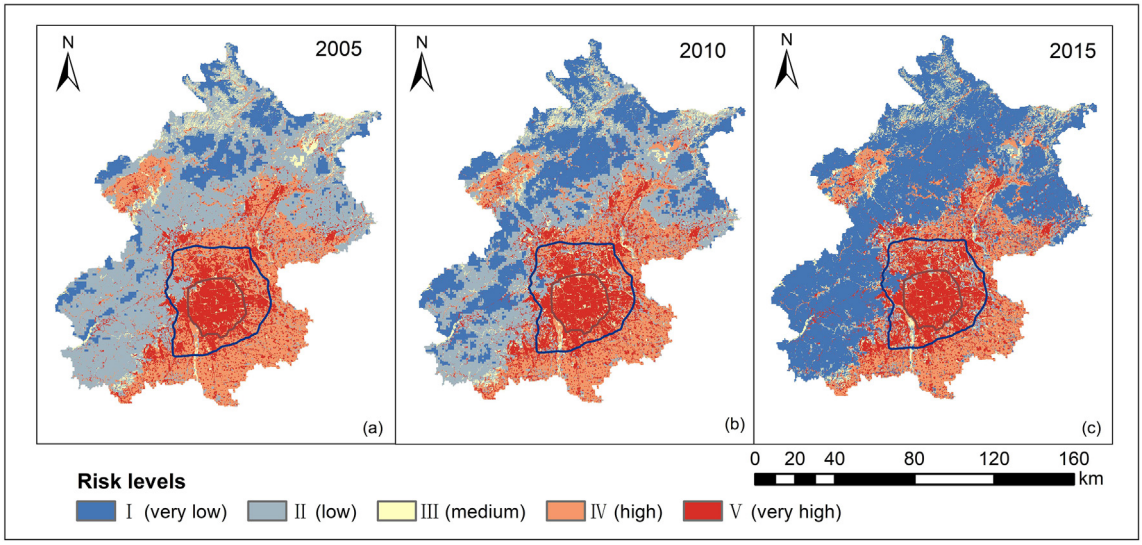

Fig. 3. Ecological risk levels in Beijing in 2005, 2010, and 2015.

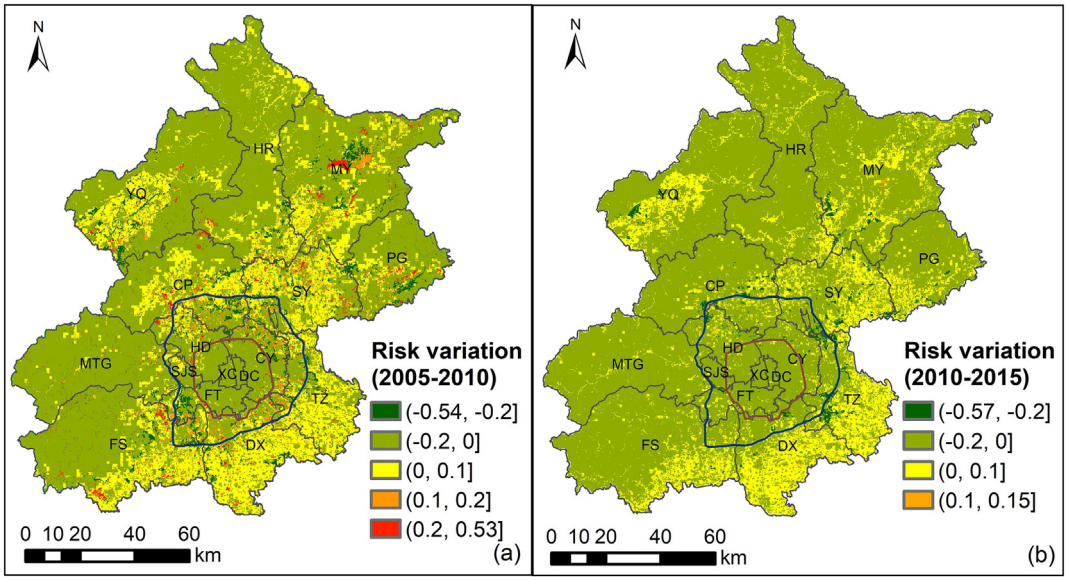

Fig. 4. Changes in ecological risks in Beijing for two periods in 2005–2015.

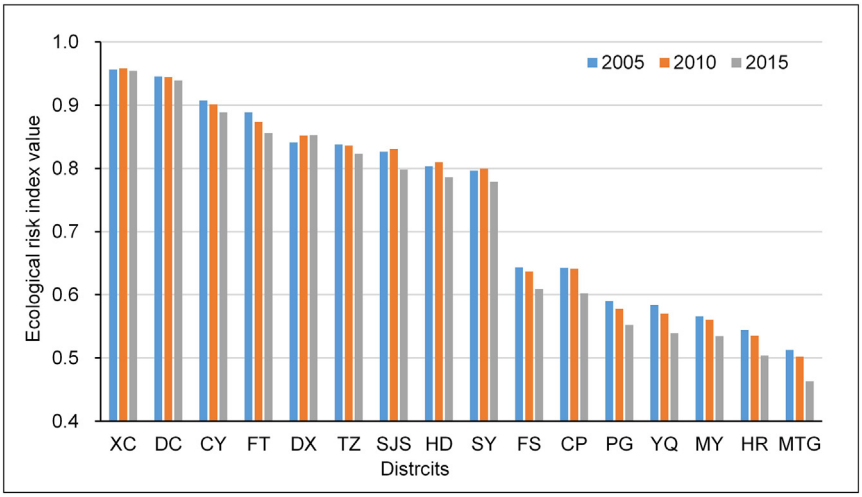

Fig. 5. Average ecological risks of districts in Beijing in 2005, 2010, and 2015.

weak. Second, variations in the model residuals (reflected by the distance between the two ends of a box or between the upper and lower whisker limits in a box plot) became increasingly smaller in all the three years when ISC increased from 30% to 70%, indicating that the linear relationship between ecological risk and ISC became increasingly stronger. Third, the R^2 of the linear regression models apparently increased (from 0.04–0.15 to 0.12–0.19, Fig. 7-d), and the variations in the model residuals showed continuously decreasing trends when ISC increased from 70% to 90%, indicating that the accuracy of the linear regression models became much higher. Finally, variations in the model residuals became considerably small, and the R^2 of the models became very high (approximately 0.77) when ISC was over 90%, indicating a very strong linear relationship between ecological risk and ISC. Therefore, ISC thresholds for the four categories of ecological risk control strategies were 30%, 70%, and 90%, respectively.

3.3.2. Ecological risk control strategies

3.3.2.1. Category 1 with the ISC range of 90%–100%. The ISC range of this category was mainly distributed in urban areas of Beijing, including most

Table 3
Area proportions of pixels where ecological risk increased and land cover types were converted to impervious surface (IS) in Beijing for the two periods in 2005–2015.

	2005–2010			2010–2015		
Ecological risk increase	Area of pixels where risk increased (km^2)	Area of pixels where risk increased and land cover types were converted to IS (km^2)	Area proportion	Area of pixels where risk increased (km^2)	Area of pixels where risk increased and land cover types were converted to IS (km^2)	Area proportion
(0, 0.1]	3898.17	7.97	0.20%	2949.51	13.62	0.46%
>0.1	723.80	472.55	65.29%	45.68	32.43	70.99%

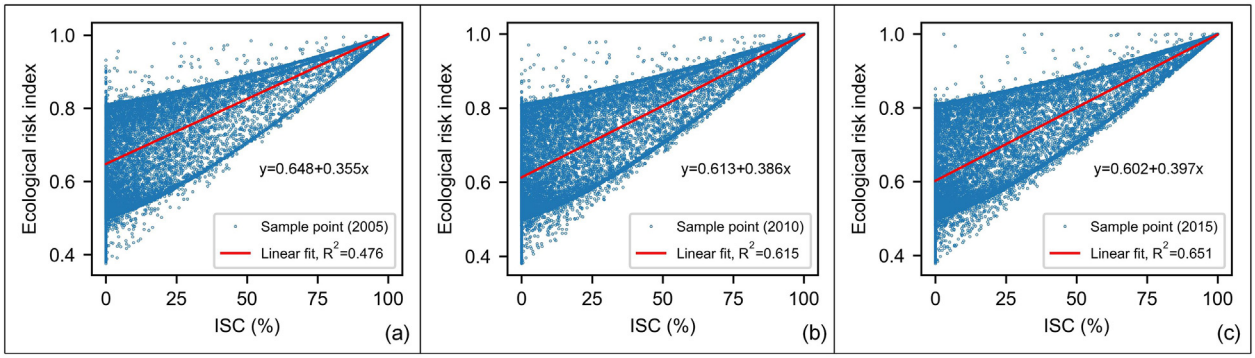

Fig. 6. Relationships between ISC and ecological risk index in Beijing in 2005, 2010, and 2015.

of the Dongcheng and Xicheng Districts; the southern part of the Haidian, Chaoyang, and Shijingshan districts; the eastern part of the Fengtai District; and the comparatively small built-up areas of the other 10 districts (Fig. S1 in the Supplementary Material). The linear regression relationship between the ecological risk index and ISC was very strong in this ISC range (Fig. 7). Therefore, reducing ISC is the most important measure for reducing ecological risks (Table 4). Although reducing ISC is difficult in areas where ISC is very high, its practicability is largely increased in Beijing because of "Beijing's Five-year Urban Renewal Action Plan (2021–2015)", which takes urban ecological restoration as one of the targets.

One commonly used measure to reduce ISC and increase vegetation coverage is to build green infrastructure. Many studies and practices show that green infrastructure can provide critical ecosystem services, such as flood regulation, urban heat island effect mitigation, and recreation in urban areas (Meerow and Newell, 2017), and thus can largely reduce ecological risks. This measure is especially important in the urban areas of Beijing because the dense population and intensive socioeconomic activity can greatly benefit from the ecosystem services provided by the green infrastructure. Moreover, because some brownfields with high ISC remain in urban areas of Beijing, such as abandoned factories, changing brownfields to green spaces or blue spaces can also effectively reduce ecological risks.

3.3.2.2. Category 2 with the ISC range of 70%–90%. The spatial distribution of the ISC range of this category is similar to that of Category 1, as the ISC of 70%–90% was mostly distributed in the periphery of the ISC of 90%–100% (Fig. S1 in the Supplementary Materials). Variations in the residuals of the linear regression models between ISC and the ecological

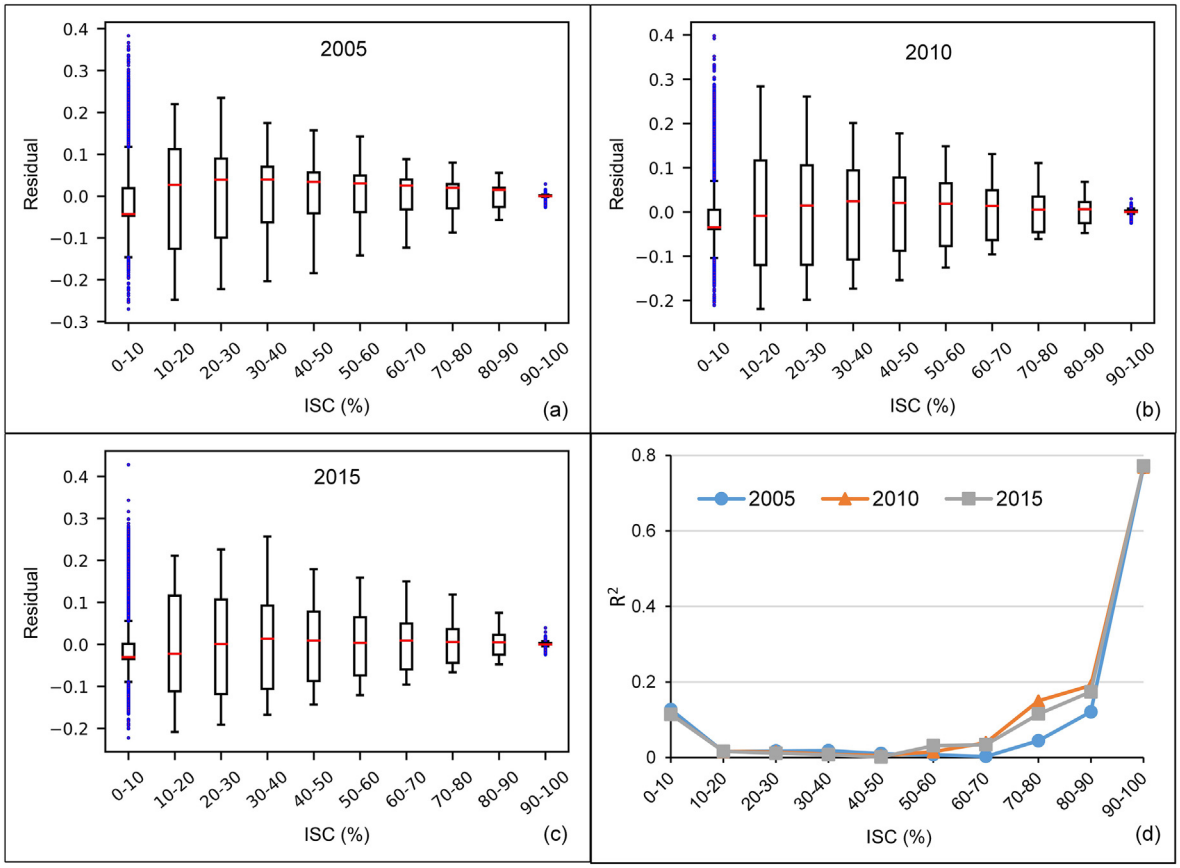

Fig. 7. Residuals and R^2 of the linear regression models between ISC and the ecological risk index in Beijing in 2005, 2010, and 2015. Diagrams a to c show the box plots of the residuals of the linear models for different ISC intervals and diagram d shows the R^2 of the models. The red lines in the boxes indicate the mean values and the blue points indicate the outliers.

Table 4
Categories of ecological risk control strategies for ISC ranges in Beijing.

Categories of ecological risk control strategies	ISC ranges and characteristics of the linear regression models between ISC and the ecological risk index
Category 1 Strategies: Reducing ISC is the most important measure to reduce ecological risks, due to the considerably strong linear regression relationship between ISC and ecological risk. Other measures only make very limited contributions to ecological risk reduction.	ISC range: 90%–100% Variations in residuals of the linear regression models were considerably small; the R^2 of the models was very large.
Category 2 Strategies: Impervious surface control measures, such as strictly controlling its expansion, are important to control ecological risks. Other measures, such landscape configuration optimization, are also necessary.	ISC range: 70%–90% Variations in residuals of the linear regression models continuously declined with the increase in ISC; the R^2 of the models largely increased.
Category 3 Strategies: Some impervious surface control measures are necessary, because the strength of the linear regression relationship between ISC and the ecological risk index continuously increased with the increase in ISC. Other measures that reduce ecological risks could become important.	ISC range: 30%–70% Variations in residuals of the linear regression models continuously declined with the increase in ISC; and the R^2 of the models was very low.
Category 4 Strategies: Controlling ecological risks mostly relies on measures other than impervious surface control, such as increasing the area proportion of forests in vegetations, because the linear regression relationship between ISC and ecological risk index was very weak.	ISC range: 0%–30% Variations in residuals of the linear regression models were very large (Fig. 7, a–c); and the R^2 of the models was very low (Fig. 7, d).

risk index continuously declined with the increase in ISC, and the R^2 of the models largely increased in this ISC range (Fig. 7). Therefore, impervious surface control measures remain important for controlling ecological risks, and other measures are also necessary (Table 4).

First, the measures applied to reduce ISC for Category 1 are also important for that in Category 2. Moreover, because this ISC range was mostly distributed on the periphery of the ISC range of 90%–100% and likely to be replaced by the latter in the urban sprawl process, controlling the expansion of impervious surfaces through, for example, setting urban growth boundaries in land use planning, is important. Landscape configuration optimization is another important measure in addition to controlling impervious surfaces. One effective strategy to reduce ecological risks caused by impervious surfaces is changing built-up areas from a concentrated spatial pattern to a dispersed spatial pattern to allow for the buffering of adverse ecological processes, such as surface runoff and pollutant wash-off (Yang and Lee, 2021). Moreover, to reduce the risk of the urban heat island effect, a significant urban ecological risk, changing dispersedly distributed small greenspaces to fewer and larger greenspaces has been shown to be effective in Beijing (Li et al., 2012).

3.3.2.3. Category 3 with the ISC range of 30%–70%. The ISC range of this category was scattered on the plain of Beijing (mainly in the six urban districts and six suburban districts; Fig. S1 in the Supplementary Material). Although the R^2 of the linear regression models was very low in this ISC range, the strength of the linear correlation between ISC and the ecological risk index continuously increased with the increase in ISC (Fig. 7). Therefore, other measures that can reduce ecological risks are important, and some IS control measures remain necessary (Table 4).

First, the measures used to control the expansion of impervious surfaces and reduce ISC for Categories 1 and 2 can also be used for Category 3. For reducing urban flooding, which exhibits a high risk in summer in Beijing, some landscape configuration optimization measures are effective. One measure is to transform impervious surfaces with medium density into discontinuously connected impervious surfaces with high–low–high density in the regions where urban renewal will be implemented (Yu et al., 2019). Another measure is to increase landscape complexity and diversity by evenly distributing different land use types in urban areas (Wu and Zhang, 2017). Moreover, placing greenspace downstream of the impervious surface is highly effective in reducing the runoff amount (Yang and Lee, 2021). In addition to these landscape configuration optimization measures, dispersedly discharging some surface runoff into permeable land can reduce the amount of runoff and pollutants directly discharged into rivers through pipes (Chen et al., 2018).

3.3.2.4. Category 4 with the ISC range of 0%–30%. The ISC of this category was mainly distributed in the suburban and rural areas on the plain and in the mountainous areas of Beijing (Fig. S1 in the Supplementary Material). Variations in residuals of the linear regression models were very large, and R^2 values of the models were very low in this ISC range (Fig. 7), indicating that the linear regression relationship between ISC and the ecological risk index was very weak. Therefore, reducing ISC will unlike decrease ecological risks, and risk control mostly relies on other measures (Table 4).

The most effective measure to reduce the ecological risks in this ISC range is to increase the area proportions of forests and water bodies, because these two ecosystem types exhibit very high equivalent factor values of several ecosystem service types (Table 1). The Beijing municipal government has implemented large-scale afforestation on the plain since 2012 (Hu et al., 2020). The planted forests have increased the provision of ecosystem services in a large part of Beijing. However, managers should be aware of the large differences in the provisioning capacities of ecosystem services (e.g., water flow regulation) among tree species and thus carefully choose the appropriate tree species in the afforestation project (Baptista et al., 2018; Yang et al., 2019). For increasing waterbody coverage, an important measure is to build wetland parks, which act as recreational sites for residents and provide many regulating services, such as flood regulation and local climate regulation. This measure has become much more feasible than it was several years ago, because of the large amount of water provided to Beijing through the South-to-North Water Diversion Project (Wan et al., 2016).

4. Discussions

4.1. Spatial-temporal dynamics of ecological risks

In Beijing, there were much fewer areas with ecological risk increases over 0.1 in 2005–2010 than in 2010–2015 (Table 3, Fig. 4); this phenomenon occurs because the increase in impervious surface area was much smaller (increased by 1.9%) in the latter period than in the former period (an increase of 13.9%). As we have demonstrated, impervious surface expansion was the main cause of the relatively large increase in ecological risk. Notably, the increasing rate of the urban population was 12.5% in 2010–2015 (Beijing Municipal Bureau of Statistics, 2021), which was much larger than that of the impervious surface area. These phenomena imply that the urbanization of Beijing was much slower in 2010–2015 than in 2005–2010 and was mainly in the form of "population urbanization" rather than "land urbanization" (Wang et al., 2016).

Regarding spatial variation in ecological risks, the mountainous areas exhibited a much lower risk level than the plain areas (Fig. 3). This phenomenon is observed because the mountainous areas were dominated by forests, and the plain areas were mainly covered by cropland and impervious surfaces (Fig. 1). As shown in Table 1, forests provide much more total ESV than cropland and impervious surfaces, substantially reducing ecological risks.

Regarding the changes in ecological risk levels from 2005 to 2015, the high level was replaced by the very high level in some areas (mainly within the 5th and 6th Ring Road) on the plain, and the low level was replaced by

the very low level in many areas in the mountains (Table 2 and Fig. 3). Moreover, the ecological risk for a large area of cropland exhibited small increases (≤ 0.1; Fig. 4), although the risk level did not increase.

There are two major reasons for these changes. The first reason is that the expansion of the impervious surface, the equivalent factors of which are zero, by occupying cropland on the plain areas (Fig. 1) resulted in a decrease in ESV (Fig. 2-a) and an increase in ecological risks in areas occupied by the expanded impervious surface. The second reason is that the NDVI increased on forested land in the mountainous areas from 2005 to 2015 and decreased on much cropland in the plain areas during the same period (Fig. S2 in the Supplementary Material). As explained in the Supplementary Material (Eqs. (3) and (4)), the equivalent factors of eight ecosystem types were modified based on the NDVI such that a higher NDVI results in larger equivalent factors, leading to lower ecological risks. Our finding that the NDVI is positively correlated with ecosystem services and negatively correlated with ecological risks is similar to that of other studies (De Carvalho and Szlafsztein, 2019; Yu et al., 2020).

4.2. Influence of impervious surface on ecological risks

Regarding the influences of impervious surfaces, the main cause of the relatively large increases in the ecological risks from 2005 to 2015 was the conversion from other land cover types to impervious surfaces (Table 3). This finding is reasonable because the equivalent factors of all ecosystem service types of impervious surfaces are the lowest (zero) among all land cover types (Table 1). A large reduction in ESV occurs when other land cover types are changed to impervious surfaces, causing a large ecological risk increase. This finding is similar to those of Liao et al. (2017) and Kang et al. (2018). Additionally, the large ecological risk increases mainly occurred on the peripheries of impervious surfaces on the plain areas in 2005–2010 (Fig. 4-a). This phenomenon can be explained by the apparent impervious surface expansion (the area increased by 13.9%) during this period (Fig. 1). This phenomenon indicates a significant trade-off between ecosystem services and urban development in rapidly urbanizing regions (Kang et al., 2019).

Thresholds of the influence of ISC on ecological risks need to be determined to categorize risk control strategies (Schuele, 1994). Studies have found ISC thresholds for influences on the urban heat island effect, runoff, water quality, and ecosystem quality in urban areas or watersheds (Brun and Band, 2000; Stepenuck et al., 2002; Wang, 2007; Guo et al., 2019). These studies have demonstrated that the adverse environmental or ecological effects increase quickly as ISC increases when ISC is within a certain range. However, the strength of the correlation between ISC and the ecological risk index exhibited a general increasing trend with the increase in ISC and did not show tipping points in this study (Fig. 6). Therefore, we identified the ISC thresholds according to the goodness of fit of the linear regression models to data in different ISC ranges (Fig. 7). We used these thresholds to determine whether controlling the impervious surface is effective for risk control for different strategy categories.

4.3. Advantages of the formulation of the ecological risk control strategies and limitations

As we have demonstrated, although the ecological risk in mountainous areas in Beijing decreased from 2005 to 2015, urban districts and several suburban districts exhibited relatively large risk values (Fig. 4); thus, developing ecological risk control strategies for Beijing is necessary. Therefore, we proposed differentiated ecological control strategies for the strategy categories and showed the spatial locations of the categories using a map (Table 4 and Fig. S1 in the Supplementary Material). Such work can help managers implement risk control countermeasures with high effectiveness in distinct regions in Beijing, for example, avoiding wasting resources when controlling the impervious surface in areas with an ISC range of 0%–30%, because the correlation between ISC and the ecological risk index is very low in this range. The advantage of differentiating strategy categories has been demonstrated in the literature, for example, Meng et al. (2015) proposed countermeasures for ecological risk management for different risk degrees, ecosystems, and risk sources in Ordos. Second, such work can demonstrate to managers where distinct ecological risk control strategies should be implemented in Beijing. Managers need a map showing the spatial distributions of strategy categories, such that provided in the Supplementary Material of this article. Third, although ISC may change temporally (Kang et al., 2018), managers can continuously adjust the strategies for regions with ISC changes by using a checklist of the risk control strategies differentiated by the ISC range and an updated map of ISC ranges.

Despite the advantages we have demonstrated, the formulation of ecological risk control strategies in this study has limitations. We only analyzed the quantitative relationship between impervious surfaces and ecological risks. Therefore, we only have first-hand scientific evidence to determine the strategy categories based on ISC and propose the controlling strategies for impervious surfaces. Nevertheless, we did not estimate the influence of other factors, such as landscape patterns. To manage this limitation, we based the proposal of the strategies, other than controlling impervious surfaces, on evidence from the literature. For example, we suggested changing the dispersedly distributed small greenspace to fewer and larger greenspaces to reduce the risk of the urban heat island effect for the ISC range of 70%–90%, because such countermeasures were shown to be effective in Beijing (Li et al., 2012). The evidence on the effects of the other strategies from the literature increases our confidence in the rationality of proposing these strategies for ecological risk control in Beijing.

Moreover, our method and data input have limitations. One limitation is the use of the equivalent factors of ecosystem services, which has been provided in the literature and was based on expert opinions (Xie et al., 2008), to evaluate ESV. Such a method results in uncertainties, especially when factor values from the literature are for the entire country and may not be suitable for Beijing. To cope with this problem, we referred to the literature (Xie et al., 2017; Xing et al., 2020) and used the NDVI and precipitation data of Beijing and China to modify the equivalent factors so that the equivalent factor values were suitable for Beijing. Another limitation is the use of the entropy weight method to determine the weights of ecosystem service types. According to this method, the weight of an ecosystem service type only depends on the dispersion of the service value in the entire sample (all the pixels of the study area), excluding the actual importance of the service to individuals (Li et al., 2021). Considering this limitation, we performed a sensitivity analysis of the major parameters used to calculate the ecological risk index. The results show that the weights of ecosystem service types make small contributions to the sensitivity (Fig. S4 in the Supplementary Material), indicating that the uncertainty of the weights exerts a small influence on the risk index values. The major limitation of the data is the use of land cover spatial data with a resolution of 30 m. We used this resolution because no finer land cover spatial data for Beijing were available for all three years. The 30 m resolution may not capture the complexity and high heterogeneity of the landscape pattern in regions where rapid land cover conversion occurs, such as the areas between the 5th and 6th Ring Road of Beijing. Therefore, we did not analyze the influence of the fragmentation and shape of impervious surfaces on ecological risks in this study.

5. Conclusions

This study aimed to demonstrate the spatial-temporal dynamics of ecological risks, reveal the influences of impervious surfaces, and formulate strategies for controlling ecological risks in rapidly urbanizing regions. To achieve these objectives, we used Beijing as a case study area, characterized the ecological risks based on ESV, mapped the levels and temporal changes in ecosystem service values and ecological risks, identified the ecological risk increases caused by impervious surface expansion, analyzed the relationship between ISC and the ecological risk index, and proposed ecological risk control strategies for the strategy categories. We found the following: (1) The mountainous areas of Beijing mainly exhibited low levels of ecological risks, and the plain areas mainly showed high risk levels. Much forested land in the mountainous areas showed increases in ESV and small decreases

in ecological risks; a large area of cropland on the plain exhibited small ESV decreases and slight risk increases from 2005 to 2015. Moreover, the urban and suburban districts exhibited much higher average ecological risks than the rural districts; (2) the expansion of impervious surfaces was the main cause of the relatively large ecological risk increases from 2005 to 2015; (3) the strategies for ecological risk control could be divided into four categories based on the division of ISC with 30%, 70%, and 90% as the thresholds; and (4) reducing ISC is the most important measure to reduce ecological risks for the category with the ISC range of 90%–100%, and increasing the area proportions of forests and water bodies is the most effective countermeasure for the category with the ISC range of 0%–30%. For the other two categories, controlling ISC and other strategies are both necessary for risk control.

Our findings indicate the large spatial and temporal dynamics of ecological risks in rapidly urbanizing regions and provide evidence of the tipping points of the influences of ISC on ecosystem services and ecological risks. Moreover, the results show that differentiating ecological risk control strategies for distinct categories in different parts of a region can enable the effective implementation of these strategies. Our study can increase the understanding of the influence of impervious surfaces on ecological risks in rapidly urbanizing regions and help inform the formulation of strategies for controlling the ecological risks in Beijing. Further studies may examine the influences of other strategies, such as landscape pattern optimization, on ecological risks in rapidly urbanizing regions.

CRediT authorship contribution statement

Ying Hou: Conceptualization, Methodology, Formal analysis, Writing – original draft. **Wenhao Ding:** Data curation, Methodology, Investigation, Writing – review & editing. **Changfeng Liu:** Conceptualization, Data curation, Methodology, Investigation, Writing – original draft. **Kai Li:** Writing – review & editing. **Haotian Cui:** Methodology, Writing – review & editing. **Baoyin Liu:** Writing – review & editing. **Weiping Chen:** Conceptualization, Funding acquisition, Project administration, Writing – review & editing.

Declaration of competing interest

The authors declare that they have no known competing financial interests or personal relationships that could have appeared to influence the work reported in this paper.

Acknowledgements

This work was supported by the Chinese Ministry of Science and Technology (2017YFC0505702) and the National Natural Science Foundation of China (41807510). The authors would like to thank Professor Weiqi Zhou and Dr. Wenjuan Yu for the land cover data support and the anonymous reviewers for the valuable comments and suggestions.

Appendix A. Supplementary data

Supplementary data to this article can be found online at https://doi.org/10.1016/j.scitotenv.2022.153823.

References

Alberti, M., Booth, D., Hill, K., Coburn, B., Avolio, C., Coe, S., Spirandelli, D., 2007. The impact of urban patterns on aquatic ecosystems: an empirical analysis in Puget lowland sub-basins. Landsc. Urban Plan. 80, 345–361.

Bai, X., Shi, P., Liu, Y., 2014. Society: realizing China's urban dream. Nature 509, 158–160.

Baptista, M.D., Livesley, S.J., Parmehr, E.G., Neave, M., Amati, M., 2018. Variation in leaf area density drives the rainfall storage capacity of individual urban tree species. Hydrol. Process. 32, 3729–3740.

Bartolo, R.E., van Dam, R.A., Bayliss, P., 2012. Regional ecological risk assessment for Australia's tropical rivers: application of the relative risk model. Hum. Ecol. Risk. Assess. 18, 16–46.

Beijing Municipal Bureau of Statistics, 2021. Beijing Statistical Yearbook 2020. China Statistics Press, Beijing.

Bell, C.D., Tague, C.L., McMillan, S.K., 2019. Modeling runoff and nitrogen loads from a watershed at different levels of impervious surface coverage and connectivity to storm water control measures. Water Resour. Res. 55, 2690–2707.

Bian, G., Du, J., Song, M., Xu, Y., Xie, S., Zheng, W., Xu, C., 2017. A procedure for quantifying runoff response to spatial and temporal changes of impervious surface in Qinhuai River basin of southeastern China. Catena 157, 268–278.

Brun, S.E., Band, L.E., 2000. Simulating runoff behavior in an urbanizing watershed. Comput. Environ. Urban. Syst. 24, 5–22.

Chen, Y., Yu, X., Zheng, S., Ziqi, Z., 2018. Control index of impervious surface in sponge city based on eco-hydrological response. China Water Wastew. 34, 116–121 (in Chinese).

Collins, S.L., Carpenter, S.R., Swinton, S.M., Orenstein, D.E., Childers, D.L., Gragson, T.L., Grimm, N.B., Grove, J.M., Harlan, S.L., Kaye, J.P., Knapp, A.K., Kofinas, G.P., Magnuson, J.J., McDowell, W.H., Melack, J.M., Ogden, L.A., Robertson, G.P., Smith, M.D., Whitmer, A.C., 2011. An integrated conceptual framework for long-term social—ecological research. Front. Ecol. Environ. 9, 351–357.

Costanza, R., D'Arge, R., de Groot, R., Farber, S., Grasso, M., Hannon, B., Limburg, K., Naeem, S., O'Neill, R.V., Paruelo, J., Raskin, R.G., Sutton, P., van den Belt, M., 1997. The value of the world's ecosystem services and natural capital. Nature 387, 253–260.

De Carvalho, R.M., Szlafsztein, C.F., 2019. Urban vegetation loss and ecosystem services: the influence on climate regulation and noise and air pollution. Environ. Pollut. 245, 844–852.

Dietz, M.E., Clausen, J.C., 2008. Stormwater runoff and export changes with development in a traditional and low impact subdivision. J. Environ. Manag. 87, 560–566.

Estoque, R.C., Murayama, Y., Myint, S.W., 2017. Effects of landscape composition and pattern on land surface temperature: an urban heat island study in the megacities of Southeast Asia. Sci. Total Environ. 577, 349–359.

Graham, R.L., Hunsaker, C.T., Oneill, R.V., Jackson, B.L., 1991. Ecological risk assessment at the regional scale. Ecol. Appl. 1, 196–206.

Guo, L., Liu, R., Men, C., Wang, Q., Miao, Y., Zhang, Y., 2019. Quantifying and simulating landscape composition and pattern impacts on land surface temperature: a decadal study of the rapidly urbanizing city of Beijing, China. Sci. Total Environ. 654, 430–440.

Heenkenda, M.K., Bartolo, R., 2016. Regional ecological risk assessment using a relative risk model: a case study of the Darwin harbour, Darwin, Australia. Hum. Ecol. Risk. Assess. 22, 401–423.

Hu, T., Li, X., Gong, P., Yu, W., Huang, X., 2020. Evaluating the effect of plain afforestation project and future spatial suitability in Beijing. Science China Earth sciences 63, 1587–1598.

Izadikhah, M., Saeidifar, A., Roostaee, R., 2014. Extending TOPSIS in fuzzy environment by using the nearest weighted interval approximation of fuzzy numbers. J. Intell. Fuzzy Syst. 27, 2725–2736.

Kang, P., Chen, W., Hou, Y., Li, Y., 2018. Linking ecosystem services and ecosystem health to ecological risk assessment: a case study of the Beijing-Tianjin-Hebei urban agglomeration. Sci. Total Environ. 636, 1442–1454.

Kang, P., Chen, W., Hou, Y., Li, Y., 2019. Spatial-temporal risk assessment of urbanization impacts on ecosystem services based on pressure-status - response framework. Sci. Rep. 9, 16806.

Kuang, W., Yang, T., Yan, F., 2018. Examining urban land-cover characteristics and ecological regulation during the construction of Xiong'an New District, Hebei Province, China. J. Geogr. Sci. 28, 109–123.

Li, X., Zhou, W., Ouyang, Z., Xu, W., Zheng, H., 2012. Spatial pattern of greenspace affects land surface temperature: evidence from the heavily urbanized Beijing metropolitan area, China. Landsc. Ecol. 27, 887–898.

Li, K., Hou, Y., Andersen, P., Xin, R., Rong, Y., Skov-Petersen, Hans, 2021. Identifying the potential areas of afforestation projects using cost-benefit analysis based on ecosystem services and farmland suitability: A case study of the Grain for Green Project in Jinan, China. Science of the Total Environment 787, 147542.

Liao, J., Jia, Y., Tang, L., Huang, Q., Wang, Y., Huang, N., Hua, L., 2017. Assessment of urbanization-induced ecological risks in an area with significant ecosystem services based on land use/cover change scenarios. Int. J. Sustain. Dev. World Ecol. 25, 448–457.

Liu, C., Chen, W., Hou, Y., Ma, L., 2020. A new risk probability calculation method for urban ecological risk assessment. Environ. Res. Lett. 15, 24016.

Lü, Y., Wang, C., Cao, X., 2018. Ecological risk of urbanization and risk management. Acta Ecol. Sin. 38, 359–370 (in Chinese).

Luo, X., Jiang, P., Yang, J., Jin, J., Yang, J., 2021. Simulating PM2.5 removal in an urban ecosystem based on the social-ecological model framework. Ecosyst. Serv. 47, 101234.

Meerow, S., Newell, J.P., 2017. Spatial planning for multifunctional green infrastructure: growing resilience in Detroit. Landsc. Urban Plan. 159, 62–75.

Meierdiercks, K.L., Kolozsvary, M.B., Rhoads, K.P., Golden, M., McCloskey, N.F., 2017. The role of land surface versus drainage network characteristics in controlling water quality and quantity in a small urban watershed. Hydrol. Process. 31, 4384–4397.

Meng, J., Xiang, Y., Yan, Q., Mao, X., Zhu, L., 2015. Assessment and management of ecological risk in an agricultural–pastoral ecotone: case study of Ordos, Inner Mongolia, China. Nat. Hazards 79, 195–213.

Qi, S., Guo, J., Jia, R., Sheng, W., 2020. Land use change induced ecological risk in the urbanized karst region of North China: a case study of Jinan city. Environ. Earth Sci. 79, 280.

Schuele, T.K., 1994. The importance of imperviousness. Watershed Protection Techniques. 1, pp. 100–101.

Shi, Y., Wang, R., Huang, J., Yang, W., 2012. An analysis of the spatial and temporal changes in Chinese terrestrial ecosystem service functions. Chin. Sci. Bull. 57, 2120–2131.

Stepenuck, K.F., Crunkilton, R.L., Wang, L., 2002. Impacts of urban landuse on macroinvertebrate communities in southeastern Wisconsin streams. J. Am. Water Resour. Assoc. 38, 1041–1051.

Su, W., Duan, H., 2017. Catchment-based imperviousness metrics impacts on floods in Niushou River basin, Nanjing City, East China. Chin. Geogr. Sci. 27, 229–238.

Thom, J.K., Szota, C., Coutts, A.M., Fletcher, T.D., Livesley, S.J., 2020. Transpiration by established trees could increase the efficiency of stormwater control measures. Water Res. 173, 115597.

Walsh, C.J., Webb, J.A., 2016. Interactive effects of urban stormwater drainage, land clearance, and flow regime on stream macroinvertebrate assemblages across a large metropolitan region. Freshw. Sci. 35, 324–339.

Walsh, C.J., Fletcher, T.D., Ladson, A.R., 2005. Stream restoration in urban catchments through redesigning stormwater systems: looking to the catchment to save the stream. J. N. Am. Benthol. Soc. 24, 690–705.

Wan, W., Yin, J., Zhao, J., Lei, X., Liao, W., Qin, T., 2016. Sustainability evaluation of Beijing water deployment model before and after South-to-North Water Diversion. South-to-North Water Transfers and Water Science & Technology. 14, pp. 62–69 (in Chinese).

Wang, L., 2007. Watershed urbanization and changes in fish communities in southeastern Wisconsin streams. J. Am. Water Resour. Assoc. 36, 1173–1189.

Wang, R., Ouyang, Z., 2012. Social-economic-natural complex ecosystem and sustainability. Bull. Chin. Acad. Sci. 27, 337–345 (in Chinese).

Wang, C., Wang, B., Wang, X., 2016. Study on population urbanization and land urbanization allometric growth in China based on the structure. China Popul. Resour. Environ. 26, 135–141 (in Chinese).

Wang, Z., Zhang, L., Li, X., Li, Y., Fu, B., 2021. Integrating ecosystem service supply and demand into ecological risk assessment: a comprehensive framework and case study. Landsc. Ecol. 36, 2977–2995.

Wu, J., Zhang, P., 2017. The effect of urban landscape pattern on urban waterlogging. Acta Geograph. Sin. 72, 444–456 (in Chinese).

Xian, G., Crane, M., 2006. An analysis of urban thermal characteristics and associated land cover in Tampa Bay and Las Vegas using Landsat satellite data. Remote Sens. Environ. 104, 147–156.

Xie, G., Zhen, L., Lu, C., Xiao, Y., Chen, C., 2008. Expert knowledge based valuation method of ecosystem services in China. J. Nat. Resour. 23, 911–919 (in Chinese).

Xie, G., Zhang, C., Zhen, L., Zhang, L., 2017. Dynamic changes in the value of China's ecosystem services. Ecosyst. Serv. 26, 146–154.

Xie, T., Wang, M., Chen, W., Uwizeyimana, H., 2018a. Impacts of urbanization and landscape patterns on the earthworm communities in residential areas in Beijing. Sci. Total Environ. 626, 1261–1269.

Xie, T., Wang, M., Su, C., Chen, W., 2018b. Evaluation of the natural attenuation capacity of urban residential soils with ecosystem-service performance index (EPX) and entropy-weight methods. Environ. Pollut. 238, 222–229.

Xing, L., Hu, M., Wang, Y., 2020. Integrating ecosystem services value and uncertainty into regional ecological risk assessment: a case study of Hubei Province, Central China. Sci. Total Environ. 740, 140126.

Xu, H., Lin, D., Tang, F., 2013. The impact of impervious surface development on land surface temperature in a subtropical city: Xiamen, China. Int. J. Climatol. 33, 1873–1883.

Yang, B., Lee, D., 2021. Urban green space arrangement for an optimal landscape planning strategy for runoff reduction. Land 10, 897.

Yang, K., Pan, M., Yang, R., Song, Y., Meng, C., 2016. Water environmental impacts of impervious surfaces and control measures in Dianchi Lake Basin, China. Chin. J. Environ. Eng. 10, 5407–5412 (in Chinese).

Yang, X., Tang, L., Jia, Y., Liu, J., 2018. Ecological risk assessment of the southern Fujian Golden triangle in China based on regional transportation development. Sustainability 10, 1861.

Yang, B., Lee, D.K., Heo, H.K., Biging, G., 2019. The effects of tree characteristics on rainfall interception in urban areas. Landsc. Ecol. Eng. 15, 289–296.

Yang, T., Zhang, Q., Wan, X., Li, X., Wang, Y., Wang, W., 2020. Comprehensive ecological risk assessment for semi-arid basin based on conceptual model of risk response and improved TOPSIS model-a case study of Wei River Basin, China. Sci. Total Environ. 719, 137502.

Young, O.R., Berkhout, F., Gallopin, G.C., Janssen, M.A., Ostrom, E., van der Leeuw, S., 2006. The globalization of socio-ecological systems: an agenda for scientific research. Glob. Environ. Chang. 16, 304–316.

Yu, W., Zhou, W., Qian, Y., Yan, J., 2016a. A new approach for land cover classification and change analysis: integrating backdating and an object-based method. Remote Sens. Environ. 177, 37–47.

Yu, Y., Zhu, J., Wu, S., Zhou, S., Li, B., 2016b. Assessment of land ecological risks driven by multi-sources: a case study of Sheyang County, Jiangsu Province. J. Nat. Resour. 31, 1264–1274 (in Chinese).

Yu, H., Zhao, Y., Fu, Y., 2019. Optimization of impervious surface space layout for prevention of urban rainstorm waterlogging: a case study of Guangzhou, China. Int. J. Environ. Res. Public Health 16, 3613.

Yu, T., Bao, A., Xu, W., Guo, H., Jiang, L., Zheng, G., Yuan, Y., Nzabarinda, V., 2020. Exploring variability in landscape ecological risk and quantifying its driving factors in the amu Darya Delta. Int. J. Environ. Res. Public Health 17, 79.

Zhang, Y., Harris, A., Balzter, H., 2015. Characterizing fractional vegetation cover and land surface temperature based on sub-pixel fractional impervious surfaces from Landsat TM/ETM. Int. J. Remote Sens. 36, 4213–4232.